Journal of Environmental Science and Public Health
doi: 10.26502/jesph.96120058

Volume 3, Issue 2 **Research Article**

Spatial Analysis of Lead in the Street Dust of Mexico City: Implications for Human Health

Aguilera A[1,2], Bautista F[1*], Delgado C[3], Gogichaichvili A[3], Cejudo R[3], Gutiérrez-Ruiz ME[4], Ceniceros-Gómez AE[4], López-Santiago NR[4]

[1]Laboratorio Universitario de Geofísica Ambiental, Centro de Investigaciones en Geografía Ambiental, Universidad Nacional Autónoma de México, Michoacán, México

[2]Posgrado en Ciencias Biológicas, Universidad Nacional Autónoma de México, México

[3]Laboratorio Universitario de Geofísica Ambiental, Instituto de Geofísica, Universidad Nacional Autónoma de México, Michoacán, México

[4]Laboratorio de Biogeoquímica Ambiental, Facultad de Química, Universidad Nacional Autónoma de México, México

[*]Corresponding Author: Bautista F, Antigua Carretera a Pátzcuaro No. 8701, Col. Ex Hacienda de San José de la Huerta, C.P. 58190 Morelia, Michoacán, México, Tel: 52 443 322 3869; E-mail: leptosol@ciga.unam.mx

Received: 05 March 2019; **Accepted:** 18 March 2019; **Published:** 15 April 2019

Abstract

The systematic exposure to lead (Pb) is considered a persistent health problem in Mexico. However, human health risk in the country's most populated and contaminated City has not been estimated. In order to determine the level of Pb contamination and hazard index for human health risk assessment in Mexico City, the contamination factor and human health risk indexes were calculated from 481 street dust samples, and their spatial distribution was mapped. We found a considerable average level of contamination with Pb; the contamination factor was 5.8 times higher than the background value (22 mg/kg). The most extensive areas with a high contamination level were located in the northeastern part of the city (administrative district of Gustavo A. Madero) and in the central-eastern (administrative districts of Iztapalapa-Iztacalco). The estimated daily intake of Pb through ingestion exceeded the reference value in 56% of the city, with regard to children, and in the 12% with regard to adults. It may be concluded that there is a considerable Pb contamination in Mexico City that definitively influences the health of the population being

children as the most vulnerable. Thus, it is mandatory to reduce the Pb content in Mexico City street dust in order to prevent serious health problems for more than 20 million inhabitants.

Keywords: Lead loading; Street dust loading; Geoaccumulation index; Geographical Information System; Kriging interpolation methods

1. Introduction

The World Health Organization has declared that one in every eight deaths in the world is related to air pollution [1], representing a serious environmental problem [2]. Street dust is formed by settling pollutant particles emitted into the atmosphere and soils as well as particles from the surrounding soils [3, 4], it constitutes a good surrogate of air pollution, easy to sample and manipulate, and reflects the potential risk of exposure of the population [5-7]. Lead (Pb) is one of the contaminants of major interest in the street dust because it can cause irreversible damage to neural and intellectual development and behavior, even in low concentrations [8, 9]. Children are the most susceptible to the exposure to Pb given their hand to mouth habit and their rapid growth rates [10-12]. In Mexico, the exposure to Pb is a persistent health problem, representing an enormous risk for lead-induced mild mental retardation (the incidence rate is 5.98 for every 1000 children from 0 to 4 years old), greater than neuropsychiatric conditions of any other type. It is estimated that more than 15% of children between 0 and 4 years old will have a decrease of more than five points in their intellectual coefficient (IQ) [13].

In Mexico City, there are high Pb concentrations in the environment, as a result of intense human activities [14-16]. Some authors have also reported Pb blood levels higher than the U.S. Centers for Disease Control and Prevention's upper limit, 5 µg/dL [9, 17]. Due to this, the exposure to Pb is a concern that requires attention, and human health risk assessment, for the general population, need to be done. The objective of this study was to determine a degree of contamination and hazard index for human health risk assessment due to Pb content in street dust from Mexico City. To achieve this objective the contamination factor and risk indexes for human health were calculated and mapped. For the first time in the studies of street dust contamination in Mexico City, human health risk was estimated, and a great number of samples (n=481) were used to improve map accuracy.

2. Methods

2.1 Study site

Mexico City and its coinciding urban areas make up the third largest urban region in the world, accommodating more than 20 million habitants and more than 40,000 small and medium industries. Approximately 40 million liters of combustible fossil fuels are consumed daily, which results in tons of contaminants being emitted into the environment [18]. The northern area of the study site included an important industrial center with a high-density population (Figure 1). The central area was comprised of the historic and socioeconomic center of the city, which is highly urban and commercial. The southern area was dominantly residential and commercial. The street dust sampling was done during the dry season (March-April) of 2017. The mean temperature was 16°C, with a minimum

of 8 y maximum of 26°C. The mean relative humidity was 48%. The wind direction was 176 Azimut degrees (south) and the mean wind speed was 2.19 m/s [19]. In the urban area of Mexico City, without the southern part that has mountainous geography, 481 samples of street dust were collected from a systematic sampling. The distance of separation was approximately 1 km and was limited to 1 m^2 above the surface of the streets along the sidewalks. Rocks, leaves, and branches were removed, then the street dust was collected with a plastic brush and deposited in Polyethylene bags which were labeled and geographically referenced.

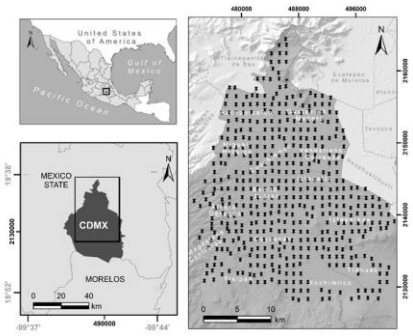

Figure 1: Map of the locations in Mexico City and the sites where samples of street dust were taken.

2.2 Geochemical analysis

In the laboratory, the samples were dried for two weeks in the shade at environmental temperatures to avoid oxidation of the minerals. Afterward, the samples were sifted through a sieve with apertures of 250 μm. The weights of the samples were registered for later calculations. The concentrations of Pb in street dust were determined by inductively coupled plasma-optical emission spectroscopy (ICP-OES). The street dust samples were weighed (0.4 g) and digested with 20 ml of concentrated HNO_3 in a Microwave Digestion System ETHOS Easy (Milestone Inc) using Teflon PFA vessels. The temperature was raised to 175 ± 5°C in approximately 5 min and it was maintained for another 4.5 min. After cooling, the digested samples were filtered using a Whatman No. 42 filter paper and were thereafter transferred into a 50 mL flask and brought to volume with Type A water [20]. Quality controls for the acid digestion method included reagent blanks, duplicate samples, and spiked samples. The quality assurance and quality control (QA/QC) results did not show signs of contamination nor loss in any of the analyses. The digestions and quality controls were analyzed in triplicate by ICP-OES spectrometer (Agilent Technologies 5100) [21]. To prepare the calibration curve the standard certified with multiple elements QCS-26R (High Purity brand) were utilized. The radio frequency potency (RF power) was 1.2 kW, the nebulization flow 0.7 L/min and the argon plasma flow 12.0 L/min. The detection limit was 0.03 mg/L (3.75 mg/kg) and the quantification limit was 0.12 mg/L (15 mg/kg).

2.3 Contamination index

A descriptive statistical analysis of the concentration of Pb, street dust and Pb loadings (mg/m^2) was completed. The Pb loading in the street dust (mg/m^2) was calculated multiplying the concentration of Pb (mg/kg) and the street dust loading expressed in kg/m^2. The level of contamination was estimated with the contamination factor (*CF*) (Equation 1). It is a quotient of the Pb concentration in the sample (C_n) and the background value (B_n).

$$CF = \frac{C_n}{B_n} \quad (1)$$

The background value indicates the average concentration of natural sources on the site. We used a background value of 22 mg/kg, quantified by Morton-Bermea et al. [22]. They collected samples in uncontaminated rural grounds outlying the city and in green urban areas at a depth of 60 to 200 cm. CF less than 1 indicates insignificant contamination, between 1-3 moderate, between 3-6 considerable, and more than 6 indicates high contamination [14]. The Geoacumulation index (I_{geo}) was also calculated to evaluate the level of contamination. Unlike the CF, the I_{geo} considers a factor of 1.5 for possible variations in the background value that may be attributed to lithogenic variations in the samples. I_{geo} was calculated by Equation 2:

$$I_{geo} = log_2\left[\frac{C_n}{1.5\ x\ B_n}\right] \quad (2)$$

The interpretation of the Igeo was: <0 (uncontaminated), 0-1 (uncontaminated to moderately contaminated), 1-2 (moderately contaminated), 2-3 (moderately to highly contaminated), 3-4 (highly contaminated), 4-5 (highly to very highly contaminated), >5 (very highly contaminated) [23-26].

2.4 Spatial analysis

Identification of the geographic patterns of the distribution of contaminants is important to understand their behavior [27]. Kriging interpolations have been widely used because they are robust and minimize the error [14, 28, 29]. The geostatistical analysis consisted of three stages: 1) exploratory analysis (statistic) of the data to identify outliers because kriging interpolations are susceptible to these values; 2) structural or spatial analysis to calculate the spatial autocorrelation, the semivariogram was computed and adjusted to a theoretical model; 3) interpolation of the data. The kriging interpolation equations can be found elsewhere [14, 29]. During the exploratory analysis, a positive asymmetric distribution of frequencies for street dust loading was observed, which brought about a logarithmic transformation and an adjustment of the data to normalize them. Thereafter, in the structural analysis, an experimental semivariogram was constructed to quantify the spatial dependency. This analysis was done with Gamma Design Software [30]. We decided to use kriging indicator method to identify contamination hotspots. For this type of interpolation, the observed $I(x)$ value become indicative codes with the function $I(x; z_k)$, under a cut-off value of z_k:

$$I(x;\ z_k) = \begin{cases} 1, & if\ z(x) \le z_k \\ 0, & otherwise \end{cases} \quad (3)$$

We chose as cut-off value the third quartile (Q3) of the frequency distribution because it represents the last 25% of the greatest values. In the case of Pb concentrations, the Q3 was 143.7 mg/kg, 6.5 times greater than the background value, which is indicative of a high level of contamination. Furthermore, the Q3 came close to the value determined by the Canadian Soil Quality Guidelines for the Protection of Environmental and Human Health (140 mg/kg). This value was employed by Delgado et al. [31] as their cut-off in their interpolations in Mexico City. In the case of street

dust loading, we obtained a better spatial autocorrelation and decided to use ordinary kriging to observe the general spatial distribution pattern. The mean error (ME) was used to determine the degree of bias in the estimates and it was calculated from:

$$ME = \frac{1}{n}\sum_{i=1}^{n} \hat{Z}(x_i) - Z(x_i) \quad (4)$$

Where, n is the number of samples, $\hat{Z}(x_i)$ is the estimated and $Z(x_i)$ is the measured value of Pb concentration, street dust loading, and Pb loading. The closer the ME is to zero, the more accurate the interpolation is [28, 32]. The raster interpolations were taken to the ArcMap Software, version 10.2 [33]. An intersection between the categories greater than the third quartile of the Pb concentrations and Pb loadings was carried out to identify the most contaminated sites. The intersection was realized with the tool "Algebra of maps". The areas with the highest Pb concentrations, street dust, and Pb loadings and greatest exposure were calculated with the function "Zonal" which is found in the toolbox for spatial analysis in ArcMap. The projection used was UTM, zone 14, Worldwide Geodesic system 84 (WGS84).

2.5 Human health risk assessment

The population exposure to Pb present in street dust can be brought about by three principal pathways: ingestion, inhalation and by absorption through the skin. In this study, the calculation of quotients of non-carcinogenetic risk due to the exposure to Pb in the street dust of Mexico City was achieved using the model developed by the United States Environmental Protection Agency for children and adults [34]. The estimated daily intake (*EDI*) in mg/kg per day by ingestion (EDI_{ing}), inhalation (EDI_{inh}), and dermal contact (EDI_{dermal}) is shown using the following equations (Equation 5, 6 and 7):

$$EDI_{ing} = \frac{C * IngR * EF * ED}{BW * AT} * 10^{-6} \quad (5)$$

$$EDI_{inh} = \frac{C * InhR * EF * ED}{PEF * BW * AT} \quad (6)$$

$$EDI_{dermal} = \frac{C * SA * AF * ABF * EF * ED}{BW * AT} * 10^{-6} \quad (7)$$

Where *C*: is the concentration of Pb in each sample site (mg/kg). *IngR*: rate the of ingestion, 100 mg/day for children and 50 mg/day for adults [35]. *EF*: frequency of exposure, 350 days/year for children and adults [34], we consider the same EF for all the sampling points because there are houses all over the city. *ED*: duration of exposure, 6 years for children and 24 years for adults [34]. *BW*: body weight, 15 kg for children and 70 kg for adults [11, 36]. *AT*: average time, 365 days for children and adults [37]. *InhR*: the rate of inhalation, 7.6 m^3/day for children and 12.8 m^3/day for adults [38]. *PEF*: the rate of particle emission, 1.36 × 109 m^3/kg [34]. *SA*: the surface of exposed skin, 2800 cm^2 for children and 5700 cm2 for adults [34]. *AF*: adherence factor, 0.2 mg/cm^2 for children and 0.07 mg/cm^2 for adults [34]. *ABF*: absorption factor (dermal), 0.001 for children and adults [34, 39]. The hazard quotients of

ingestion, inhalation and dermal contact ($HQ_{ing\ /\ inh\ /\ derm}$) for each sample point are found by dividing the into the reference dose (*RfD*) as demonstrated in equation 8:

$$HQ_{ing/inh/derm} = \frac{EDI_{ing/inh/derm}}{RfD} \quad (8)$$

The *RfD* that was applied in this study was 3.5×10^{-3} mg/kg day, calculated from the limit of tolerance for weekly ingestion, (25 µg kg bw) recommended by the World Health Organization [40]. Other authors, as Reis et al. [12], have used a much more protective *RfD* (0.03×10^{-03} mg/kg day). However; to avoid overestimating the risk, because we did not measure Pb bioaccessibility; we used the *RfD* most commonly cited in the literature [11, 36, 41, 42]. The hazard index (HI) is presented as the sum of the *HQ* for the three exposure pathways: ingestion, inhalation and dermal contact. The HI can evaluate the human health risk, if it is greater than 1, it is possible that non-carcinogenic effects may occur; if the HI value is less than 1 the opposite may be expected [34]. As Pb is considered as a possible carcinogen [43, 44] the incremental lifetime cancer risk (*ILCR*) was calculated with the following equation:

$$ILCR = EDI_{ing/inh} * CSF_{ing/inh} \quad (9)$$

The cancer slope factor for ingestion (CSF_{ing}) was 0.0085 mg/kg/day, and for inhalation CSF_{inh} was 0.042 mg/kg/day [45]. The acceptable or tolerable risk is over the range of 1E-06 to 1E-04 [34]. Subsequently, the *HQ* that were higher than the value of 1 were interpolated utilizing the kriging indicator method. The threshold value was 1, indicating that the *ADD* was greater than the *RfD*.

3. Results and Discussion

3.1 Contamination index

To evaluate the contamination level for Pb in the street dust, the contamination factor (CF) was calculated. We found an average CF of 5.8, which indicates considerable contamination, while the maximum reached an extremely high level of contamination (CF=86.7). According to the CF, 31% of the samples were at a level of very high contamination, 45% were considerable, 21% were moderate and only 3% of the samples were in a category of insignificant contamination. We found an average I_{geo} of 1.6, which indicates a moderate contamination level. The maximum value reached a very high level of contamination (I_{geo}=5.9), but only the 1% of the samples were in this category: very high contaminated, 7% were highly contaminated, 23% was from moderately to highly contaminated, 45% was moderately contaminated, 17% was from uncontaminated to moderately contaminated and the remaining 7% was uncontaminated.

In Mexico City, the average contamination level with Pb in the street dust was from moderately (I_{geo}=1.6) to considerable (FC=5.8). This means that the natural content of Pb has increased due to anthropogenic activities in the City. This was also observed by the positive asymmetric distribution of frequencies of the Pb concentrations and the Pb loading (standardized bias and kurtosis >2) (Table 1). An asymmetric frequency distribution is usually encountered in the studies of environmental contamination for those elements of anthropogenic origin, given that the

concentrations depend on the distance from the sources [14, 27, 46, 47]. These results agree with the findings of previous researches in topsoil from Mexico City [14, 15, 48]. In those investigations, it was reported that the origin of Pb was, principally, anthropogenic and came from historical pollution from the use of leaded gasoline in the past.

n=481	Street dust loading (g/m^2)	Concentration of Pb (mg/kg)	Pb loading (mg/m^2)
Average	46.5	127.9	5.5
Median	44	101.2	4.2
Standard Deviation	23.2	134.6	5.1
Coefficient of Variation	0.5	1.1	0.9
Minimum	5.4	8.8	0.1
Maximum	173.3	1907.8	52.8
Q3	143.7	59.7	6.8
Standardized Bias	8	60.2	31.5
Standardized Curtosis	7.8	324.2	96.3

Table 1: Statistic description of street dust loading, concentration and Pb loading.

The contamination level with Pb in Mexico City would seem to have decreased from the only previous study done for street dust to ours. In the previous research [31] the average concentration of Pb was 206 mg/kg, and in ours, it was 128 mg/kg (Table 2). However, the maximum concentration of Pb in the present study (1908 mg/kg) was greater than that in the previous one (610 mg/kg). Because of this, it is essential to continue to observe Pb contamination. In both studies, the average concentrations of Pb in street dust were slightly greater than the concentrations reported from soils in Mexico City, when comparing similar techniques, XRF or ICP (Table 2). Bi et al. [49] has also observed that Pb concentrations in street dust were higher than those in soils. In fact, these authors consider that street dust could become a source of potentially toxic elements to urban soils.

Reference	Season	Matrix	Technique	n	Average (mg/kg)	Minimum	Maximum
[22]	Summer and spring	Soil	ICP-MS	135	112	5	452
[15]	Spring	Soil	XRF-WD	146	116	15	693
[14]	Spring	Soil	XRF-ED	89	163	20	654
[31]	Spring	Dust	XRF-ED	89	206	17	610
This Study	Spring	Dust	ICP-OES	481	128	9	1908

ICP-OES- inductively coupled plasma-optical emission spectroscopy; ICP-MS-inductively coupled plasma mass spectroscopy; XRF-WD-X-ray fluorescence by wave longitude; XRF-ED-X-ray fluorescence by dispersive energy.

Table 2: Average concentrations of Pb in street dust and soils in Mexico City.

3.2 Spatial analysis

The Pb concentration, street dust, and Pb loadings were represented by exponential models (Table 3). The first two variables had a coefficient of determination (r^2) bigger than 0.9, but the Pb loading had an r^2 of 0.4. The structural variance that was explained by the models ranged between 60 and 90%, the rest of the variance was an error or noise and it is known as nugget variance.

Variable	Model	Nugget Variance (%)	Structural Variance (%)	Range (m)	Model r^2	Mean Error
Pb concentration KI	Exponential	10	90	1980	0.90	5.1
Street dust loading KO	Exponential	40	60	59760	0.98	0.2
Pb loading KI	Exponential	9	91	2040	0.40	3.0

KI-kriging indicator; KO-kriging ordinary

Table 3: Statistics of semivariogram models describing the spatial variability.

The range represents the distance of influence of the autocorrelation. For Pb concentrations and Pb loadings, the ranges were 1980 and 2040 m, respectively. The street dust loading range was much wider, 59760 m, this could indicate that the autocorrelation extends beyond the sampled area. The mean error was close to zero for the street dust loading, however, it was greater for the Pb concentrations and loadings, 5.1 and 3, respectively. To corroborate the Pb concentration and Pb loading interpolations, we displayed on the maps the sampling points by quartile categories. All the samples in the highest probability of exceed the third quartile (Q3) category were effectively higher than Q3 (Figure 2 and 4).

3.2.1 Concentrations of Pb (mg/kg): The areas with the highest concentrations of Pb, those that exceeded the Q3 (143.7 mg/kg), which is a high level of contamination, according to the CF, were distributed throughout Mexico City. However, the most extensive areas were located in the northeast, in the administrative districts of Gustavo A. Madero, and in the northwest of Iztapalapa (Figure 2). The surface with Pb concentrations greater than 140 mg/kg was much smaller than in the only previous study of street dust in Mexico City [31]. We believe that the number of samples made the difference; while we used 481 samples, they used 89; therefore, our map was more precise and could distinguish in greater detail the areas with a high level of contamination. We consider that showing more accurate areas is an advantage of our maps, as this precision allows the stakeholders to identify the priority sites that require attention.

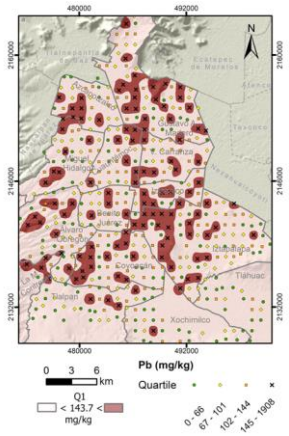

Figure 2: Spatial distribution of Pb concentrations in street dust in Mexico City.

3.2.2 Street dust loading (g/m^2): The greatest quantities of street dust were located in the eastern part of the city, principally in Iztapalapa and Tláhuac, between 43 and 80 g/m^2. It would seem that in the sites closest to the periphery it was possible to find greater street dust loading, probably because the street dust is not removed and accumulates with the time. Moreover, the eastern part is on an ex-lake surface and the sediments can easily be transported (Figure 3). The center of the city had lower quantities than the eastern, between 30 y 42 g/m^2, while the lowest quantities of street dust were found in the southeast of the city, between 17 and 29 g/m^2, in Tlalpan and Coyoacán. The resultant interpolation appropriately represented the general pattern of spatial distribution; however, it had a smoothing effect that occasioned an underestimation of the highest values and overestimation of the lowest.

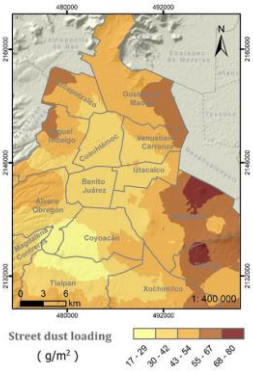

Figure 3: Spatial distribution of street dust loading per m^2 in Mexico City.

3.2.3 Pb loading (mg/m^2): The most extensive areas with Pb loading greater than Q3=6.8 mg/m^2 were located in the eastern part of the city (Figure 4), principally in the districts of Gustavo A. Madero and Iztapalapa. We did not have a Pb loading reference value to find out the level at which a site could be considered as contaminated; however, as the Q3 for Pb concentrations corresponded to a high level of contamination, we assumed that Q3 could represent the highest contamination with Pb loading.

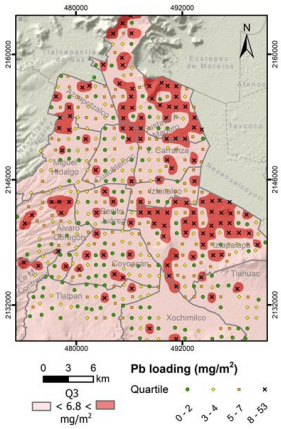

Figure 4: Spatial distribution of Pb loading in Mexico City.

The only reference value for Pb loading that we found was the permitted Pb loading limit in the house dust set by the U.S. Environmental Protection Agency [50], which is 0.43 mg/m^2. Ninety-eight percent of the samples were greater than this limit and the Q3 was 15.8 times higher. This could seem a very high value, however, a reference value for street dust Pb loading is needed for proper comparison.

3.2.4 Highest level of Pb concentration and Pb loading

The superimposition of the areas with the highest concentrations and Pb loadings, more than Q3, permitted us to distinguish the sites with the highest level of contamination, due to both Pb concentrations and Pb loadings (Figure 5). The most extensive areas with a high level of contamination were in the northeastern part of the city (Gustavo A. Madero) and in the northwestern part of the Iztapalapa district. With this map, we also corroborated that street dust is a good surrogate of air pollution, as other authors said [5], even better than soils. In a study undertaken in Mexico City in 2004, it was observed that the greatest concentrations of Pb in the air were located in the northeastern part of the city [17]; our results also showed the highest level of contamination with Pb from street dust in the northeastern.

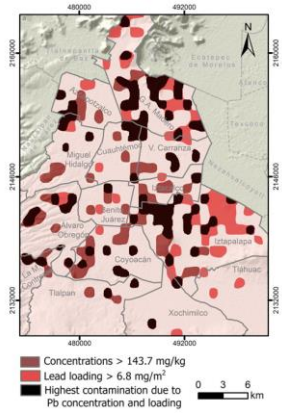

Figure 5: Areas of highest contamination: high concentrations and Pb loading in Mexico City.

3.3 Human health risks

We founded a tolerable risk to develop cancer during a lifetime. The average $ILCR_{ing}$ was between the tolerable risk range of 1E-06 to 1E-04 [34], for children and adults. Only nine samples exceed this range for children, with a maximum $ILCR_{ing}$ of 6.2E-04, and only one sample exceeded the range for adults, that was the maximum value of 2.7E-04 (Table 4). Due to Pb inhalation, the $ILCR_{inh}$ was below the tolerable risk range for all the samples. The maximum values, for children and adults, were 1.7E-07 and 2.5E-07, respectively. In the case of non-carcinogenic risk, the average HI was greater than 1, for children (Table 4). Therefore, possible adverse effects for human health may occur. For adults, the average HI was less than 1, however, 11% of the samples exceed this limit. The principal exposure pathway to Pb was the ingestion of street dust, both for children and adults. In fact, HQ_{ing} contributed the most to the HI, while HQ_{inh} and HQ_{derm} contributed little. For children, the average HQ_{ing} value was 1.4 with a maximum of 20.8. For adults, the HQ_{ing} was 0.6 with a maximum of 9. More than half of the samples, that is 56%, had an HQ_{ing} greater than 1, for children, and 12% for adults. In other studies ingestion was also the main exposure pathway to Pb [11, 24, 25, 36, 39], followed by dermal contact and lastly by inhalation. However, none of these last two routes had hazard quotients greater than 1, signifying that they do not represent a significant risk.

	Children					**Adults**				
	HQ_{ing}	**HQ_{inh}**	**HQ_{derm}**	**HI**	**$ILCR_{ing}$**	**HQ_{ing}**	**HQ_{inh}**	**HQ_{derm}**	**HI**	**$ILCR_{ing}$**
Average	1.4	7.8E-05	7.8E-03	1.4	4.2E-05	0.6	1.1E-04	5.E-03	0.6	1.8E-05
Median	1.1	6.2E-05	6.2E-03	1.1	3.3E-05	0.48	9.0E-05	4.E-03	0.5	1.4E-05
Minimum	0.1	5.4E-06	5.4E-04	0.1	2.9E-06	0.04	8.0E-06	3.E-04	0.0	1.2E-06
Maximum	20.8	1.2E-03	0.12	21	6.2E-04	9	1.7E-03	0.07	9	2.7E-04

HQ_{ing}-hazard quotient of ingestion; HQ_{inh}-hazard quotient of inhalation; HQ_{derm}-hazard quotient of dermal contact; HI-hazard index; $ILCR_{ing}$-incremental lifetime cancer risk of ingestion; $ILCR_{inh}$-incremental lifetime cancer risk of inhalation.

Table 4: Risk assessment of Pb in street dust for children and adults.

The HQ_{ing} for children were greater than for adults, which was expected given that the rate of ingestion in children is higher because of their lower body weights [36]. Children are also more vulnerable to exposure to Pb because of where they play, which represents a greater risk for the ingestion of contaminated street dust [39]. Furthermore, children are less tolerant of toxins than are adults [36]. We mapped the spatial distribution of HQ_{ing} instead of HI because HQ_{ing} was the main exposure pathway and it represents 99% of the HI (Table 4). For children, the map demonstrated that there were areas of health risk in all of the districts studied, with quotients greater than 1 (Figure 6). These values were obtained from concentrations of 91 mg/kg and on.

In fact, empirical investigations have indicated that the concentrations of Pb in the soil should be ~40 mg/kg to assure Pb levels in the blood less than 5 µg/dL, the limit set by the U.S. Centers for Disease Control and Prevention's [8]. Even more, this limit should be more deeply analyzed since negative affections on intelligence and

behavior in children have been reported [13]. In Mexico City, our findings indicated that negative affections in children may be expected due to Pb exposure. Furthermore, some authors have reported Pb blood levels higher than 5 µg/dL in the city [9, 17], then the affections on intelligence and behavior in children could be expected [13]. Children in the northeastern had Pb blood levels 11% higher than those who lived in the southeastern part of the city [17]. Due to this, negative affections on children's health should be deeply studied.

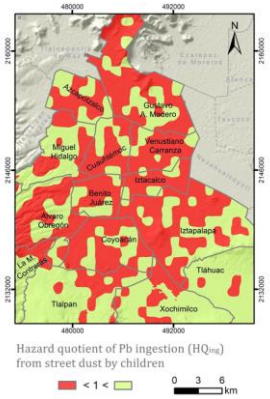

Figure 6: Spatial distribution of HQing of street dust by children in Mexico City.

In the case of HQ_{ing} for adults, there were significantly fewer areas that surpass the threshold of 1 (Figure 7). The largest extensions are located in the northeastern part of Iztapalapa, the southeastern part of Gustavo A. Madero, and the eastern part of Coyoacan.

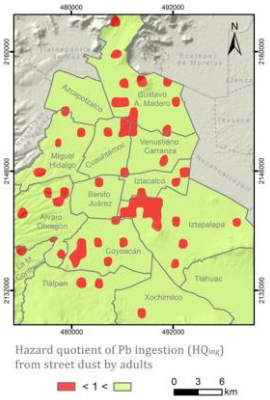

Figure 7: Spatial distribution of HQing of street dust by adults in Mexico City.

It is important to remember that the estimated daily intake calculated in this study are only estimations, based on factors of general exposure. For example, the rate of ingestion per day applied to all of the sampled sites was that reported by the United States Environmental Protection Agency [35], but this varies according to the street dust loading present in each site. Furthermore, not all of the Pb found in the samples is assimilated by the organism, and it is, therefore, important to measure the bioaccessibility of Pb in street dust to adjust the HQ [10, 12, 41]. On the other hand, other potential sources, such as soils, water, and foods, have not been considered, all or some of which

could elevate the HQ [42]. What our results indicate is that high HQ_{ing} are alert signals, especially for children, and more studies should be performed.

4. Conclusions

The concentrations of Pb in street dust have been altered in Mexico City by human activities, producing a considerable increase in the level of lead in the environment (contamination factor 5.6, I_{geo} 1.6). Thanks to the versatility of geographic information systems and interpolation models, it was possible to identify the most contaminated areas in which there are high lead concentrations and lead loadings. This study is first tentative to quantify the lead loading in street dust. This analysis in combination with the concentrations of lead allows having firm constraints about the population's exposure to lead contamination. Namely, we clearly identified that the areas of greatest exposure were located in the districts of Gustavo A. Madero and Iztapalapa. Children were found to be at higher health risk, since in 56% of the cases the hazard index was greater than the admitted safety level, while for adults it was 12%. The ingestion of street dust was the principal route of exposure, for both children and adults.

Funding

This work was supported by the Secretary of Science, Technology, and Innovation of Mexico City with the project designated SECITI/051/2016. Anahi Aguilera thanks CONACYT for the Ph.D. Fellowship awarded to her to take part in this research.

Conflict of Interests

The authors have declared no conflict of interest.

References

1. 7 million premature deaths annually linked to air pollution. World Health Organization WHO (2014).
2. Calderón-Garcidueñas L, Reynoso-Robles R, Pérez-Guillé B, et al. Combustion-derived nanoparticles, the neuroenteric system, cervical vagus, hyperphosphorylated alpha synuclein and tau in young Mexico City residents. Environmental Research 159 (2017): 186-201.
3. Bautista F, Cram Heydrich S, Sommer Cervantes I Suelos. In Eds.: Bautista F, Palacio JL, Delfín H. Técnicas de muestreo para 20 manejadores de recursos naturales (2nd Edn.). Universidad Nacional Autónoma de México (2011): 227-258.
4. Sánchez-Duque A, Bautista F, Goguitchaichvil A, et al. Evaluación de la contaminación ambiental a partir del aumento magnético en polvos urbanos. Caso de estudio para la ciudad de Mexicali, México. Revista Mexicana de Ciencias Geológicas 32 (2015): 501-513.
5. Menezes-Filho JA, Fraga de Souza KO, Gomes Rodrigues JL, et al. Manganese and lead in dust fall accumulation in elementary schools near a ferromanganese alloy plant. Environmental Research 148 (2016): 322-329.
6. Rodrigues JLG, Bandeira MJ, Araújo CFS, et al. Manganese and lead levels in settled dust in elementary

schools are correlated with biomarkers of exposure in school-aged children. Environental Polluion 236 (2018): 1004-1013.

7. Sanleandro PM, Navarro AS, Díaz-Pereira E, et al. Assessment of heavy metals and color as indicators of contamination in street dust of a city in SE Spain: Influence of traffic intensity and sampling location. Sustainability 10 (2018).
8. Laidlaw MAS, Filippelli GM, Brown S, et al. Case studies and evidence-based approaches to addressing urban soil lead contamination. Applied Geochemistry 83 (2017): 14-30.
9. Tamayo y Ortiz M, Téllez-Rojo MM, Hu H, et al. Lead in candy consumed and blood lead levels of children living in Mexico City. Environmental Research 147 (2016): 497-502.
10. Brewer PA, Bird G, Macklin MG. Isotopic provenancing of Pb in Mitrovica, northern Kosovo: Source identification of chronic Pb enrichment in soils, house dust and scalp hair. Applied Geochemistry 64 (2016): 164-175.
11. Mohmand J, Eqani SAMAS, Fasola M, et al. Human exposure to toxic metals via contaminated dust: Bio-accumulation trends and their potential risk estimation. Chemosphere 132 (2015): 142-151.
12. Reis AP, Patinha C, Wragg J, et al. Urban geochemistry of lead in gardens, playgrounds and schoolyards of Lisbon, Portugal: Assessing exposure and risk to human health. Applied Geochemistry 44 (2014): 45-53.
13. Caravanos J, Dowling R, Téllez-Rojo MM, et al. Blood Lead Levels in Mexico and Pediatric Burden of Disease Implications. Annals of Global Health 80 (2014): 269-267.
14. Ihl T, Bautista F, Cejudo Ruíz FR, et al. Concentration of toxic elements in topsoils of the metropolitan area of Mexico city: A spatial analysis using ordinary kriging and indicator kriging. Revista Internacional de Contaminacion Ambiental 31 (2015): 47-62.
15. Rodríguez-Salazar MT, Morton-Bermea O, Hernández-Álvarez E, et al. The study of metal contamination in urban topsoils of Mexico City using GIS. Environmental Earth Sciences 62 (2011): 899-905.
16. Vega E, Ruiz H, Escalona S, et al. Chemical composition of fine particles in Mexico City during 2003-2004. Atmospheric Pollution Research 2 (2011): 477-483.
17. Schnaas L, Rothenberg SJ, Flores MF, et al. Blood lead secular trend in a cohort of children in Mexico City (1987-2002). Environmental Health Perspectives 112 (2004): 1110-1115.
18. Molina LT, Madronich S, Gaffney JS, et al. An overview of the MILAGRO 2006 Campaign: Mexico City emissions and their transport and transformation. Atmospheric Chemistry and Physics 10 (2010): 8697-8760.
19. SIMAT. Atmospheric Monitoring System (Sistema de Monitoreo Atmosférico), Mexico City (2018).
20. USEPA. Method 3051A Microwave assisted acid digestion of sediments, sludges, soils and oils (2007).
21. USEPA. Method 6010C Inductively Coupled Plasma-Atomic Emission Spectrometry (2007).
22. Morton-Bermea O, Hernandez E, Martinez-Pichardo E, et al. Mexico City topsoils: Heavy metals vs. magnetic susceptibility. Geoderma 151 (2009): 121-125.
23. Chakraborty S, Man T, Paulette L, et al. Rapid assessment of smelter/mining soil contamination via portable X-ray fluorescence spectrometry and indicator kriging. Geoderma 306 (2017): 108-119.

24. Eqani SAMAS, Khalid R, Bostan N, et al. Human lead (Pb) exposure via dust from different land use settings of Pakistan: A case study from two urban mountainous cities. Chemosphere 155 (2016): 259-265.
25. Li F, Cai Y, Zhang J. Spatial characteristics, health risk assessment and sustainable management of heavy metals and metalloids in soils from Central China. Sustainability 10 (2018).
26. Nwankwoala H, Ememu A. Contamination Indices and Heavy Metal Concentrations in Soils in Okpoko and Environs, Southeastern Nigeria. Journal of Environmental Science and Public Health 02 (2018): 77-95.
27. Tang R, Ma K, Zhang Y, et al. The spatial characteristics and pollution levels of metals in urban street dust of Beijing, China. Applied Geochemistry 35 (2013): 88-98.
28. Hernandez-Stefanoni JL, Ponce-Hernandez R. Mapping the spatial variability of plant diversity in a tropical forest: Comparison of spatial interpolation methods. Environmental Monitoring and Assessment 117 (2006): 307-334.
29. Delgado C, Pacheco J, Cabrera A, et al. Quality of groundwater for irrigation in tropical karst environment: The case of Yucatán, Mexico. Agricultural Water Management 97 (2010): 1423-1433.
30. Robertson G. GS+: Geostatistics for the Environmental Sciences. Gamma Design Software, Plainwell. Michigan, USA. (2008).
31. Delgado C, Bautista F, Gogichaishvili A, et al. Identificación de las zonas contaminadas con metals pesados en el polvo urbano de la Ciudad de México. Revista Internacional de Contaminación Ambiental 35 (2019): 81-100.
32. Hua L, Yang X, Liu Y, et al. Spatial distributions, pollution assessment, and qualified source apportionment of soil heavy metals in a typical Mineral Mining City in China. Sustainability 10 (2018).
33. ESRI. ArcGIS 10.2. Getting started with ArcGIS. Redlands, California, USA (2004).
34. USEPA. Risk Assessment Guidance for Superfund (RAGS) Volume III-Part A: Process for Conducting Probabilistic Risk Assessment, Appendix B (Vol. III). U.S. Environmental Protection Agency, EPA 540-R-02-002 (2001).
35. USEPA. Exposure Factors Handbook: 2011 Edition (2011th Edn.). Environmental Protection Agency, Washington, DC; EPA/600/R-09/052F (2011).
36. Kurt-Karakus, P. B. Determination of heavy metals in indoor dust from Istanbul, Turkey: Estimation of the health risk. Environment International 50 (2012): 47-55.
37. USEPA. Risk assessment guidance for superfund (RAGS). Volume I. Human health evaluation manual (HHEM). Part E. Supplemental guidance for dermal risk assessment (Vol. 1). U.S. Environmental Protection Agency, EPA/540/1-89/002 (1989).
38. Li X, Poon CS, Liu PS. Heavy metal contamination of urban soils and street dusts in Hong Kong. Applied Geochemistry 16 (2001): 1361-1368.
39. Ali MU, Liu G, Yousaf B, et al. Pollution characteristics and human health risks of potentially (eco)toxic elements (PTEs) in road dust from metropolitan area of Hefei, China. Chemosphere 181 (2017): 111-121.
40. WHO. WHO guidelines for drinking-water quality, (3rd Edn.) Geneva (2008).
41. Gu YG, Gao YP, Lin Q. Contamination, bioaccessibility and human health risk of heavy metals in

exposed-lawn soils from 28 urban parks in southern China's largest city, Guangzhou. Applied Geochemistry 67 (2016): 52-58.

42. Li HH, Chen LJ, Yu L, et al. Pollution characteristics and risk assessment of human exposure to oral bioaccessibility of heavy metals via urban street dusts from different functional areas in Chengdu, China. Science of the Total Environment 586 (2017): 1076-1084.
43. Canaz E, Kilinc M, Sayar H, et al. Lead, selenium and nickel concentrations in epithelial ovarian cancer, borderline ovarian tumor and healthy ovarian tissues. Journal of Trace Elements in Medicine and Biology 43 (2017): 217-223.
44. Farokhi A, Tayebipoor M, Koohpeima F, et al. Lead and cancer. Journal of Cellular Immunotherapy 3 (2017): 2.
45. OEHHA. Air Toxics Hot Spots Program Technical Support Document for Cancer Potencies. Appendix B. Chemical-specific Summaries of the Information Used to Derive Unit Risk and Cancer Potency Values. (2009).
46. Guvenç N, Alagha O, Tuncel G. Investigation of soil multi-element composition in Antalya, Turkey. Environment International 29 (2003): 631-640.
47. Pan H, Lu X, Lei K. A comprehensive analysis of heavy metals in urban road dust of Xi'an, China: Contamination, source apportionment and spatial distribution. Science of the Total Environment 609 (2017): 1361-1369.
48. Morton-Bermea O, Rodríguez-Salazar MT, Hernández-Alvarez E, et al. Lead isotopes as tracers of anthropogenic pollution in urban topsoils of Mexico City. Chemie der Erde 71(2011): 189-195.
49. Bi C, Zhou Y, Chen Z, et al. Heavy metals and lead isotopes in soils, road dust and leafy vegetables and health risks via vegetable consumption in the industrial areas of Shanghai, China. Science of the Total Environment 619-620 (2018): 1349-1357.
50. USEPA. Lead Regulations (2017).

Citation: Aguilera A, Bautista F, Delgado C, Gogichaichvili A, Cejudo R, Gutiérrez-Ruiz ME, Ceniceros-Gómez AE, López-Santiago NR. Spatial Analysis of Lead in the Street Dust of Mexico City: Implications for Human Health. Journal of Environmental Science and Public Health 3 (2019): 210-225.